Ultrafiltration of Fucus vesiculosus extracts under different operating conditions

Rui Costa (ruicosta@esac.pt)
Instituto Politecnico de Coimbra https://orcid.org/0000-0003-2488-0914
Tiago Madeira
Instituto Politecnico de Coimbra
Catarina Marçal
Universidade de Aveiro https://orcid.org/0000-0002-0861-2517
Susana M. Cardoso
Universidade de Aveiro https://orcid.org/0000-0002-7882-737X
Licínio Gando-Ferreira
Universidade de Coimbra https://orcid.org/0000-0003-0739-1238

Research Article

Keywords: Fucus vesiculosus, ultrafiltration, iodine, alginates, fucoidans, mathematical modeling

Posted Date: March 1st, 2022

DOI: https://doi.org/10.21203/rs.3.rs-1335940/v1

Abstract

The interest in separating and concentrating bioactives and minerals from seaweeds extracts is growing due to large health benefits of these substances. The aim of this study was to investigate the separation of components of *Fucus vesiculosus* seaweed extracts by tangential ultrafiltration and apply Hermia's models adapted to crossflow ultrafiltration to understand the fouling mechanism. The influence of membrane cut-off varying from 5 to 150 kDa, crossflow velocity from 0.081 and 0.095 m/s and transmembrane pressure between 2 and 8 bar was studied. The present study revealed that the ultrafiltration membranes process was successful in clarifying and still delivering permeates with a high content in iodine. Clarification was almost completely achieved with 5 kDa polyethersulfone membrane, while the hydrophilic polyethersulfone membrane was not adequate to due to the high retention in iodine. Cake layer formation mathematical model was successfully used to the predict the permeate flux over time. There was evidence that cake layer is the fouling mechanism in the filtration of *Fucus vesiculosus* extracts, whatever the membrane crossflow velocity or transmembrane pressure, probably due to the high content of these extracts in alginates.

Statement Of Novelty

Separation of valuable compounds from *Fucus vesiculosus* extracts is of great industrial importance and thus insights into its mechanisms and influence of operational parameters mechanisms that influence the separation by ultrafiltration are needed. This study enabled to sketch those to further optimize the filtration, by providing knowledge on the effect of membrane composition and influence of the operation parameters molecular weight cut-off, cross-flow velocity and transmembranar pressure. Additionally, the fouling mechanism, which knowledge is needed to further improve the filtration efficiency, was captured to be cake filtration.

1. Introduction

As part of the blue bioeconomy, the acceleration of algal exploitation in fields such as food, feed, agriculture and pharmaceutical offers unique possibilities to tackle several sustainable development goals of the 2030 Agenda [1]. The current global macroalgae market is almost exclusively settled in Asia, although there is currently an exponential trend towards their sustainable production and exploitation worldwide, mostly due to recognition of their exceptional nutritional value and health benefits [2].

Among the three major groups of algae (i.e., green algae, red algae and brown algae), the latter stand out for their abundance in the bioactive polysaccharides fucoidans and/or laminarans, the phenolic compounds phlorotannins, the pigment fucoxanthin and iodine, which have been repeatedly associated with distinct of their therapeutic properties, including the treatment of cellulite, blood clot formations, rheumatoid arthritis, asthma, atherosclerosis, diabetes, obesity, psoriasis and skin diseases, cancer and other oxidative and inflammatory related conditions [3].

Fucus vesiculosus, traditionally named as bladder wrack, is a widespread brown macroalgae, which is naturally found in cold-temperate waters, particularly in the coastlines of the North Sea, the western Baltic Sea, and the Atlantic and Pacific oceans [4]. Alike other brown macroalgae, *Fucus vesiculosus* it has been claimed to be rich in the above-mentioned bioactive compounds. In fact, this is one of the richest macroalgae-source of fucoidans, which can accumulate up to 26% of its dry weight. Moreover, due to its high iodine contents, it has been used in traditional medicine for centuries for treating goiter, i.e., the swelling of thyroid and thyroid-related complications, and obesity [5].

Inclusion in food is an attractive use of seaweeds to profit from the nutritional and health benefits of seaweeds like *F. vesiculosus*, but the overall acceptance of seaweed's taste and flavor by most western consumers still limits its use in food and thus the concentration of the benefits of seaweeds in tasteless pills is a proper strategy to benefit from the health properties of these food materials. For this, the most common strategy in the food supplements industry engages the extraction of valuable compounds with organic solvents or water, followed by their concentration and drying [6].

The separation of less valuable compounds from the valuable compounds can be done using green technologies. membrane filtration is a non-thermal process, capable of preserving of nutritional qualities contained in fluids. Overall, it can separate particles (microfiltration), molecules (ultrafiltration) to ions (nanofiltration). To separate seaweed extracts after centrifugation ultrafiltration (UF) should be considered. UF can separate particles (suspended particles, bacteria, viruses) from the rest of the fluid and fractionate molecules with molecular weight of hundreds of kDa down to the units of kDa [7]. However, in this operation, fouling, the accumulation of particles on the retentate side of the membrane, is a serious problem that must be prevented or diminished to make use of its potential, decreasing operation costs and processing time. Membrane filtration has been applied and studied in a number of application such as, among others, the phenolic compounds from fruit and vegetables [8] and seeds [9], anthocyanins and monosaccharides from grape marc extract [10] or phytosterol from orange juice [11].

Ultrafiltration of seaweeds' extracts has been used to concentrate carrageenan, agar and alginates [12]. However, to the best of the authors' knowledge, the application of membrane filtration to *Fucus vesiculosus* extract has not been studied. In this work, the influence of molecular weight cut-off of the membrane, and its processing conditions of crossflow velocity and transmembrane pressure on the ultrafiltration of *Fucus vesiculosus* extracts was studied. The type of fouling was also assessed through the application of mathematical modeling.

2. Materials And Methods

2.1 Raw material

The seaweeds from *F. vesiculosus* were cultivated in a land-based integrated multitrophic aquaculture (IMTA) system at ALGAplus Lda, a company based in Aveiro district, Portugal. After collection, the macroalgae were washed with sterilized seawater followed by centrifugation to remove excess water. The seaweed was then dried at 20 °C and milled with Retsch SK10 to particles with less than 250 µm diameter.

2.2 Preparation of extracts

Extractions were done at 120 °C in a retort (Raypa RES-75, Barcelona, Spain) for 2 h with additional 30 min to heat the sample to 120 °C and 30 min to lower the temperature to 100 °C, after which was immediately cooled down in a water bath in Schott flasks of with 1 L of distilled water (pH=6.6 at 25°C) with a proportion of seaweed per water of 50 g per liter. During the extraction were kept closed to avoid water vapour losses. The solubilized material was separated from the sediments in a centrifuge (Rotanta 460R, Germany) at 20 °C, 6780 rpm for 10 min.

Extracts used for chemical analyses were frozen at -80°C (Thermo Fisher Scientific, ULT1786-4-V41, Asheville) and freeze-dried (UNICRO MC-4L-60°C, Martinsried). The resulting dried extracts were weighted and kept in freeze up to chemical analyses.

2.3 Membrane filtration

The filtration system used was a Sepa CF II membrane system (GE Osmonics, USA) at room temperature with concentrate recirculation until a 500 mL permeate volume was obtained and starting from a 2000 mL feed solution volume, which corresponds to volumetric concentration ratio (VCR) of 1.33.

The permeate flow was measured over time at intervals of 2-3 minutes to gather data on the occurrence of fouling phenomena. The retentate leaves the titanium cell where the membrane is located and then passes through a rotameter that measures the flow of the concentrate, making it possible to control and test the system and the membrane at different flow rates. After passing through the rotameter, the retentate flows back to the feed container.

Cross-flow velocities (CFV) of 0.081 m/s and 0.095 m/s and transmembrane pressures (TMP) of 2, 5 and 8 bar were tested. The membranes used were Microdyn-Nadir (Wiesbaden, Germany) sheet membranes, of polyethersulfone with molecular weight cut-offs (MWCO) of 5 and 150 kDa, and of hydrophilic polyethersulfone with a cut-off of 50 kDa. The influence of membrane MWCO (3), transmembrane membrane pressure (3) and crossflow velocity (2) on the permeate flow rate and quality and on the retentate quality were investigated in a total of 18 (3×3×2) combinations of experimental conditions.

Membrane cleaning started with rinsing with distilled water, followed by rinsing with an organic detergent P3 Ultrasil 11 (kindly supplied by ORM, Lda.) with concentration of 50 g/L, and then again with water.

The hydraulic permeabilities were measured using distilled water at 20 °C, were 18.9, 46.8, and 57.3 L h^{-1} m^2 bar^{-1}, respectively for 5, 50 and 150 kDa. The solute retention coefficient (fraction of solute retained by the membrane) was calculated according to Eq. (1),

$$R = \left(1 - \frac{C_p}{C_f}\right) \times 100 \quad (1)$$

where C_p (g•L^{-1}) and C_f (g•L^{-1}) are the concentrations of solute in permeate and feed, respectively.

2.4 Physical analyses

2.4.1 pH

The pH meter PHM61 (Radiometer, Copenhagen) was used to measure the pH. Three measurements were made in each solution.

2.4.2 Viscosity

The viscosity measurements were performed at 25.0 ± 0.2 °C in a water bath PrecisionTerm Selecta (Barcelona) using a Cannon-Fenske (Petrotest Instruments, Dahlewitz, Germany), calibrated with water viscosity of 1.0038 mm^2/s at 20°C. Measurements were taken in 5 replicates.

2.4.3 Turbidity

The turbidity of the final permeate was measured using a turbidity meter HI 83749 (Póvoa do Varzim, Portugal), after calibration with different turbidity standards (<0.1, 15, 100 and 750 NTU). Three measurements were done in each sample. Results were expressed as nephelometric turbidity units (NTU).

2.4.4 Color

The color of the suspensions was measured instrumentally using CT-310 Chroma Meter (Minolta Camera Co. Ltd., Osaka, Japan), in the L*a*b* system, after calibration with distilled water. In this system, L* denotes lightness on a scale of 0 (black) to 100 (lightness), the a* value describes the intensity in green color (negative) and in red color (positive), and the b* value in blue color (negative) and in yellow color (positive). Triplicate measurements were taken in each suspension and the final value was presented as an average (± standard deviations).

2.5 Chemical analyses

2.5.1 Solids content

Solids' content was determined in triplicate after drying 5 g of each suspension at 105°C until constant weight.

2.5.2 Fucose content

Fucose (L-fucose) was determined using a commercial kit (L-fucose, Megabyte, Bray, Ireland). Briefly, 10 mg of extract was diluted in 1 mL of distilled water and if there were no complete dissolution samples were vortexed and filtered (0.45 mm polytetrafluoroethylene (PTFE) syringe filters). Subsequently, 200 µL of water, 10 µL of fucose extract, 40 µL of fucose kit buffer and 10 µL of nicotinamide adenine dinucleotide phosphate (NADP+) solution (supplied by the kit) were placed on a 96 polystyrene (PS) flat bottom well plate. After 4 min of incubation at room temperature, 5 µL of L-fucose dehydrogenase suspension (supplied by the kit) was added and the mixture was incubated at 37 0C for 10 min. Finally, the absorbance was measured at 340 nm using the Multiscan plate reader. Fucose was quantified using the standard supplied by the kit. The fucose content was expressed as g/ 100gseaweed.

2.5.3 Iodine content

A 7700 inductively coupled plasma mass spectrometer (ICP-MS) from Agilent Technologies, equipped with nickel sampler and skimmer cones and a collision/reaction cell was used for iodine determination. Rh was used as the internal standard. TMAH extracts were conveniently diluted before ICP-MS measurement and the dilution was varied from 1:5 to 1:20. Isotope of 127I was analysed, with 3.0 mL/min of He as the reaction gas to avoid interferences on this mass. The limit of detection (LOD) and the limit of quantification (LOQ) of the ICP-MS measurements were 0.5 and 1.3 µg/ L, respectively for I. The accuracy of our method was validated by Seronorm TM trace elements Blood L2 standard reference material. The CRM determination value for I was 86.6 ± 5.8 ng/ g, while reference value on the certificate was and 107 ± 22 ng /g.

2.6 Fouling Models

The main disadvantage of pressure-driven membrane processes is the decline in permeate flux over time due to fouling phenomena that offers additional resistance to the transport of solutes through the membrane. Therefore, it is essential to elucidate the underlying mechanism that controls membrane fouling. Hermia (1982) developed empirical models based on Eq. (2) to describe four basic types of fouling that occurs in dead-end filtration.

$$\frac{d^2t}{dV^2} = K\left(\frac{dt}{dV}\right)^n \qquad (2)$$

where V is filtrate volume, t the time, K the kinetic constant and n a parameter whose value defines the fouling type: complete blocking (n=2), partial pore blocking (n=1), internal pore blocking (n=3/2) and cake layer formation (n=0).

The general equation for Hermia's models adapted to crossflow ultrafiltration [14] is as follows:

$$-\frac{dJ}{dt} = K_{CF}\,(J - J^*)\,J^{2-n} \qquad (3)$$

where J^* is the terminal flux and K_{CF} is a constant that depends on the pressure gradient, the viscosity of the permeate, the blocked area per unit of permeate flux and the membrane resistance. Considering Eq. (3) and depending on the value, different analytical solutions can be obtained as shown in Table 1.

2.7 Statistical analyses

All measurements were made with replicates and were tested for their variance and correlation between them using the IBM SPSS Statistics statistical software (v24, IBM, Armonk, USA).

The influence of variables was studied with a two-way ANOVA. In the case it was detected an influence of a variable, the Tukey test for significant differences was applied. The level of significance applied to the tests was 0.05.

A nonlinear optimization tool of the MaLlab software, version R2015a, was used to estimate the parameters of the fouling models applied to the different filtration tests, where the goodness of each fit was evaluated through the value of the coefficient of determination (R^2).

3. Results And Discussion

3.1 Characterization of extracts

Table 2 presents the composition and physical properties of extracts of *Fucus vesiculosus* obtained after water extraction at 120°C during 2 h. Total solids extraction yield is maximum at this temperature compared to extraction at lower temperatures between 100°C and 25°C [15]. The extracts presented a high solids content (14.31%), where fucoidans can represent 25.7% [3]. Fucose content can reach 44% of fucoidans and fucoxanthin [16], making this sugar a reliable indicator of the content of these compounds. Extracts obtained in this work presented a fucose content of 3.26% (w/w). Iodine was extracted to a content of 132 mg/L or 939 mg/kg dry solids, which is an appreciable amount that enables the enrichment of food products, taking into consideration that 150 mcg/day is the recommended daily intake for an adult [17]. Iodine is the most nutritionally valuable component of these extracts and thus the clarification of the extract and the concentration of iodine are valuable outcomes of the UF process before further use to produce pills or incorporation in other food or nutraceutical products.

The extracts are cloudy and opaque corresponding to a high turbidity of 347 NTU, which is within the range of apple processing effluent [18]. *F. vesiculosus* is a brown alga and thus the extract was brown with L, a* and b* of, respectively, 85.81, -0.63 and 23.75. The viscosity of the extracts was on average 1.73 mPa·s, value within the range of viscosity that of water [19]. The pH of all extracts was within the short range 5.55-5.60.

3.2 Effect of operating conditions on permeate and retentate properties

The selection of a suitable ultrafiltration membrane is essential for the optimization of the seaweed extract filtration. The performance of three membranes with cut-off of 5 and 150 kDa of polyethersulfone (PES) and of 50 kDa of hydrophilic polyethersulfone (PESH), was characterized in terms of permeate and retentate properties, and permeate flux after a volume concentration ratio (VCR) of 1.33 (Table 3). The retention coefficients are presented in Table 4.

On the retentate side, solids content increased slightly ($P<0.05$) (Tables 2 and 3) due to the small VCR of 1.33, with no significant differences observed between the retentates of the different membranes (Table 3). Total solids were retained between 45 to 51% by the membranes tested (Table 4).

The pH of the retentate and permeate were similar to that of the feed, as well as the color parameters.

The viscosity of retentate increased slightly but significantly ($P<0.0001$) compared to the feed, between 1.85 and 2.01 mPa·s. The viscosity of the permeate decreased to 1.06 mPa·s for all MWCO, close to the viscosity of water at 20°C of 1.00 mPa·s [19].

The effect on turbidity was more disparate, being 98% retained by the 5 kDa membrane and 73-79% by the other membranes. Contradictory to the change on solids content, turbidity decreased ($P<0.05$) on the retentate side compared to the feed when lower MWCO membranes were used. This can be explained by clogging on the membrane, which may have caused solids to be removed from the feed, but were not released into the retentate, which was not enough to affect the solids content, but was enough to affect turbidity. On the permeate side, as expected, the turbidity of the permeate decreased drastically compared to that of the feed, because these were mostly kept on the retentate and on the membrane and decreased more on the smaller MWCO membrane ($P<0.05$). The turbidity of the permeate prepared with 5 kDa is close to water standards, ideally <1 NTU for aesthetic aspects [20]. Higher MWCO membranes did not produce such clear streams.

The luminosity (L) increased from the feed to the permeate, the yellow tone (b*) decreased ($P<0.05$), and the red tone (a*) not present significant changes. The b* color parameter also decreased when lower MWCO membranes were employed ($P<0.05$) resulting in a weaker yellow tone. This means that high molecular weight compounds that contribute to the brown tone, stay mainly clogged in the membrane and in the retentate.

Fucose retention varied between 4 and 64%, though no significant differences were obtained.

Iodine retention was 13-16% for the PES membranes of 5 and 150 kDa and was significantly higher for the 50 kDa PESH membrane. PES membranes have been subject of improvements of hydrophilicity (called PESH membranes) to decrease the risk of the fouling caused by the high hydrophobicity of PES, especially in protein-contacting applications (Otitoju et al., 2018). However, these membranes may present disadvantages such as a high adsorption of polyphenols from olive waste, attributed to the polar interactions with the membrane [21]. These polar interactions may also explain the higher retention of iodine in this work by the PESH membrane of 50 kDa.

Overall, the performance of the membranes differs mainly from 5 kDa to 50/150 kDa, and slightly between 50 and 150 kDa, what may be due to a lack of solids with molecular weight in the range 50-150 kDa. This is in fact the case of the ethyl acetate fraction of the aqueous layer after hexane extraction of *Fucus vesiculosus*, in which the only 15.6% of the compounds mass presented MW between 5 and 100 kDa [22].

Based on the above-mentioned parameters, the 5 kDa PES membrane should be chosen if remotion of solids and a small retention of iodine is needed. However, other operational parameters, such as permeate flux, must be considered on the design of the industrial process of filtration.

3.3 Flux modeling

The modeling of the flux during tangential filtration is essential to optimize this process for separation efficiency, energy efficiency and equipment size. Flux modeling can be done using two approaches [23]: by applying phenomenological models such as gel-polarization, osmotic pressure, resistance-in-series, and fouling models, or using non-phenomenological models, which have been used to interpret the limiting phenomena and to predict the permeate flux.

Since the main problem in filtration processes is the membrane fouling, which results in a reduction of the permeate flux, increasing costs and decreasing productivity of the operation, fouling models were used in this work. Fouling is a result of particle-particle and particle-membrane hydrophobic and electrostatic interactions and depends on several factors such as composition of the feed (specially size of components and its aggregation behavior) and of the membrane and its physical properties, ionic strength and pH of the feed, and operation parameters such as temperature, transmembrane pressure and crossflow velocity [24, 25]. Bowen et al. (1995) suggested several steps for fouling that can occur in sequence or simultaneously:

(1) complete blocking: the small pores are blocked by particles on the membrane surface.

(2) internal pore blocking: particles adsorb to the inner surfaces of large pores.

(3) intermediate blocking: particles mount on top of others on top of the membrane with others blocking some pores.

(4) cake layer formation: a cake is built along the time as pores become blocked.

Fouling models are useful to understand what kind of mechanism affects the decrease of permeate flux and further development of strategies to diminish it. In this work, 4 fouling models were applied, each one corresponding to the 4 types of fouling previously mentioned. These models were initially developed by Hermia to dead-end filtration and further transformed to be applied to tangential filtration [14].

The models listed in Table 1 were used to describe the flux decline over time for the three ultrafiltration membranes under different conditions determined by the transmembrane pressure (TMP) and crossflow velocity (CFV) values. As an example of the fitting of all models, the flux modeling results obtained for the filtration tests with different molecular weight *cut-off* membranes (MWCO), at CFV=0.095 m/s and TMP=5 bar, are depicted in Fig. 1. Analyzing Fig. 1 and R^2 values listed in Table 5, it can be observed that the best agreements between experimental and calculated values were achieved with the models 1, 2 and 4 with R^2 in the range 0.96-0.98 for the experiments with 150 and 50 kDa membranes. The results are similar for all conditions as can be seen in the supplementary material.

Although the differences in R^2 are on average 4% between models, the fittings are slightly better for model 4 (cake filtration) except for the condition 150 kDa/0.081 $m \cdot s^{-1}$ /2 bar, where model 1 (complete blocking) fitted better.

Fucus vesiculosus solids contain mainly up to 66% of carbohydrates and up to 17% of protein, depending on several environmental factors [3]. The carbohydrates include mainly alginates (up to 58.8%), then fucoidans (25.7%) and laminarians (19%). All these components are expected to be in the extract and thus to affect the filtration flux.

Filtration of alginates is a well-studied case, known to result in cake filtration [27]. The filtration flux of alginate solutions decreases rapidly, decreases faster and more if bivalent cations such Ca^{2+} are present due to cross-linking polymerization. Its three-dimensional structure is a factor the influences the formation of the gel layer. If its concentration is low (around 2 ppm), fouling occurs in two phases with pore blocking in the first phase followed by cake formation but on concentrations of 50 ppm, only cake formation was observed [25]. This could be the case of the filtrations in this work since a simple estimation of alginates in *F. vesiculosus* extracts with the contents above mentioned, can easily reach 10,000 ppm.

Fucoidans, a valuable bioactive compound present in these extracts, and the second biggest group of polysaccharides from *F. vesiculosus,* compared to alginate is not very viscous and it does not gel [28], thus it is not expected to contribute as much to the cake formation, though it can be trapped within the alginate cake.

An additional cause of cake filtration in several applications like whey filtration [24] or brewer's yeast filtration [29] are proteins, which are affected by the ionic strength and also the presence of bivalent cations. Ionic strength leads to electric double layer compression which results in weak electrostatic repulsion [30]. Also, NaCl appears to reduce intermolecular reactions, promoting binary proteins deposition on the membrane surface.

Thus, it is reasonable to expect that cake filtration in the ultrafiltration of *F. vesiculosus* extracts is prevalent particularly due to the presence of alginates and proteins.

The predictions of the flux variation with time using the model 4, for all tested filtration conditions, are shown in Fig. 2. It is visible that the calculated flux decline profiles match quite closely with the experimental data in most cases. The parameter and R^2 values for the fitting of the model 4 to the data are shown in Table 6.

A confirmation of the fouling mechanism was done by the method used by Hwang & Lin (2002). These authors plotted filtration curves of $\log(-dJ_P/dt)$ against $\log(J_P)$ and applied a regression analysis to obtain the parameter *n* of the Hermia's models (equation 2) to infer about the fouling mechanism (if close to 2, 1.5, 1 or 0 - see Table 1). An example is presented in Figure 3. The parameter *n* can be obtained from the linear region observable at the highest values on both axis for each curve. The second region corresponds to steady state flux and the slope tends infinite. Overall, the values obtained in this work are closer to zero (data not shown), confirming that the cake model is most suitable model to predict the ultrafiltration permeate flux of *Fucus vesiculosus* extracts.

3.4. Influence of MWCO, TMP and CFV

The order of magnitude of the flux and the time required for achieving its final value depends on the MWCO, TMP and CFV of the filtration process. Regarding the MWCO effect, in general it was found that permeate flux increased with membrane's

MWCO, which can be explained by the larger pore size (see Fig. 1). For instance, the initial flux for the 150 kDa membrane was of »25 L/h m^2 at CFV=0.095 m/s and TMP=5 bar and was reduced around 34%. Under the same conditions, reductions in this flux of approximately 20 and 59% were obtained for the 50 and 5 kDa membranes, respectively.

The effect of TMP has influence on the driving force of the process which determines the magnitude of the permeate flux. This effect was more evident for the 5 kDa membrane (Fig. 2). When the TMP increased from 2 to 8 bar, an increase in the initial flux of » 65% and » 54% was observed operating at 0.081 m/s and 0.095 m/s, respectively. Also, the flux decline is more significant at higher TMP. The flux was lower at 8 bar when compared to one at 5 bar for the 50 kDa and 150 kDa membranes for the lowest CFV, which shows that the membranes become more fouled at higher TMP. This can probably be justified considering that at high pressures the convective transport across the membrane becomes predominant, favoring the accumulation of solutes at the membrane surface, increasing the concentration polarization and consequently fouling tendency [14]. The concentration polarization can be reduced by increasing the CFV [32]. It was found that lower fluxes were obtained when the CFV decreased, mainly for the 50 kDa and 150 kDa membranes, as expected. The change of CFV did not have a significant effect on the flux for the 5 kDa membrane. In addition, the steady state permeate flux was attained faster operating at higher CFV.

4. Conclusions

This work enabled to understand the ultrafiltration of *Fucus vesiculosus* extracts using PES and PESH membranes. The membranes of 150, 50 and 5 kDa used were found to provide a clear separation of solids, resulting in permeates with half of the solids content and of viscosity close to water, though only the 5 kDa membrane delivered a permeate with a turbidity close to water standards.

The PES membranes of 5 and 150 kDa retained a small portion of the iodine between 13-16% but the PESH membrane retained twice as much, most probably due to the hydrophilic treatment used to produce it that may retain polar compounds. The 5 kDa PES membrane was thus the best option to filtrate these extracts, since it achieved a high clarification with minimum retention of iodine and a stable flux over time. High crossflow velocities and transmembrane pressures of 5 or 2 bar are adequate to achieve higher permeate fluxes.

The application of Hermia's models adapted to tangential filtration revealed that cake formation is the dominant fouling mechanism in the ultrafiltration of *Fucus vesiculosus* extracts. This is probably due to the high content in alginates that tend to form a gel. The cake model overall predicted well the flux over time and may be used in similar applications.

Declarations

Funding

Project CENTRO-01-0145-FEDER-023780 HEPA: Healthier eating of pasta with algae co-financed by the European Regional Development Fund (ERDF), through the partnership agreement Portugal2020 - Regional Operation Program CENTRO2020.

Foundation for Science and Technology (FCT), the European Union, the National Strategic Reference Framework (QREN), the European Regional Development Fund (FEDER), and Operational Programme Competitiveness Factors (COMPETE), the Associated Laboratory for Green Chemistry (LAQV) of the Network of Chemistry and Technology (REQUIMTE) (UIDB/50006/2020). Project PTDC/BAA-AGR/31015/2017 (Algaphlor), financed the research contract of Susana M. Cardoso.

Foundation for Science and Technology financial support to Research Centre for Natural Resources, Environment and Society - CERNAS (UID/AMB/00681/2013, UIDB/00681/2020) and Strategic Project of CIEPQPF (UIDB/00102/2020).

Acknowledgements

The authors wish to thank ALGAplus Lda for supplying the seaweed flour.

Declarations of interest: none

Data availability: The data will be available upon request.

References

1. Olavur Gregersen, Liina Joller-Vahter, John van Leeuwen, Snejana MoncheOlavur Gregersen, Liina Joller-Vahter, John van Leeuwen, Snejana Moncheva, Jens Kjerulf Petersen, Wilco Schoonderbeek, Vitor Verdelho Vieira, Helena Vieira, Maye Walravenva, Jens Kjeru, M.W.: Blue Bioeconomy Forum: roadmap for the blue bioeconomy. European Comission, Technopolis Group and Wageningen Research (2019)
2. FAO: The State of World Fisheries and Aquaculture 2020. Sustainability in action. (2020)
3. Catarino, M.D., Silva, A.M.S., Cardoso, S.M.: Phycochemical constituents and biological activities of Fucus spp. Mar. Drugs. 16, (2018). https://doi.org/10.3390/md16080249
4. GBIF: GBIF Backbone Taxonomy-Fucus vesiculosus L., https://www.gbif.org/species/8222574
5. Küpper, F.C., Feiters, M.C., Olofsson, B., Kaiho, T., Yanagida, S., Zimmermann, M.B., Carpenter, L.J., Luther III, G.W., Lu, Z., Jonsson, M., Kloo, L.: Commemorating Two Centuries of Iodine Research: An Interdisciplinary Overview of Current Research. Angew. Chemie Int. Ed. 50, 11598–11620 (2011). https://doi.org/https://doi.org/10.1002/anie.201100028
6. Neves, F. de F., Demarco, M., Tribuzi, G.: Drying and Quality of Microalgal Powders for Human Alimentation. In: Vítová, M. (ed.) Microalgae: From Physiology to Application. intechopen (2020)
7. Mulder, J.: Basic Principles of Membrane Technology. Springer Netherlands (1996)
8. Carbonell-Alcaina, C., Álvarez-Blanco, S., Bes-Piá, M.A., Mendoza-Roca, J.A., Pastor-Alcañiz, L.: Ultrafiltration of residual fermentation brines from the production of table olives at different operating conditions. J. Clean. Prod. 189, 662–672 (2018). https://doi.org/10.1016/j.jclepro.2018.04.127
9. Balyan, U., Sarkar, B.: Integrated membrane process for purification and concentration of aqueous Syzygium cumini (L.) seed extract. Food Bioprod. Process. 98, 29–43 (2016). https://doi.org/10.1016/j.fbp.2015.12.005
10. Muñoz, P., Pérez, K., Cassano, A., Ruby-Figueroa, R.: Recovery of anthocyanins and monosaccharides from grape marc extract by nanofiltration membranes. Molecules. 26, (2021). https://doi.org/10.3390/molecules26072003
11. Abd-Razak, N.H., Chew, Y.M.J., Bird, M.R.: Membrane fouling during the fractionation of phytosterols isolated from orange juice. Food Bioprod. Process. 113, 10–21 (2019). https://doi.org/10.1016/j.fbp.2018.09.005
12. Lipnizki, F., Dupuy, A.: Food Industry Applications. In: Hoek, E.M. V. and Tarabara, V. V. (eds.) Encyclopedia of Membrane Science and Technology. p. 2390. Wiley (2013)
13. Hermia, J.: Constant pressure blocking filtration laws—application to power-law non-newtonian fluids. Trans. Inst. Chem. Eng. 60, 183–187 (1982)
14. Vela, M.C.V., Blanco, S.Á., García, J.L., Rodríguez, E.B.: Analysis of membrane pore blocking models adapted to crossflow ultrafiltration in the ultrafiltration of PEG. Chem. Eng. J. 149, 232–241 (2009). https://doi.org/10.1016/j.cej.2008.10.027
15. Ferreira, R.M., Ribeiro, A.R., Patinha, C., Silva, A.M.S., Cardoso, S.M., Costa, R.: Water Extraction Kinetics of Bioactive Compounds of Fucus vesiculosus. Molecules. 24, 1–15 (2019). https://doi.org/10.3390/molecules24183408
16. Li, B., Lu, F., Wei, X., Zhao, R.: Fucoidan: Structure and bioactivity. Molecules. 13, 1671–1695 (2008). https://doi.org/10.3390/molecules13081671
17. Iodine - Health Professional Fact Sheet, https://ods.od.nih.gov/factsheets/Iodine-HealthProfessional/
18. Barter, P.J., Deas, T.: Comparison of portable nephelometric turbidimeters on natural waters and effluents. New Zeal. J. Mar. Freshw. Res. 37, 485–492 (2003). https://doi.org/10.1080/00288330.2003.9517183
19. Kestin, J., Sokolov, M., Wakeham, W.A.: Viscosity of liquid water in the range -8°C to 150°C. J. Phys. Chem. Ref. Data. 7, 941–948 (1978). https://doi.org/10.1063/1.555581

20. WHO: Guidelines for drinking-water quality, fourth edition incorporating the first addendum. World Health Organization, Geneva (2017)
21. Cassano, A., Conidi, C., Drioli, E.: Comparison of the performance of UF membranes in olive mill wastewaters treatment. Water Res. 45, 3197–3204 (2011). https://doi.org/10.1016/j.watres.2011.03.041
22. Wang, T., Jónsdóttir, R., Liu, H., Gu, L., Kristinsson, H.G., Raghavan, S., Ólafsdóttir, G.: Antioxidant capacities of phlorotannins extracted from the brown algae Fucus vesiculosus. J. Agric. Food Chem. 60, 5874–5883 (2012). https://doi.org/10.1021/jf3003653
23. Quezada, C., Estay, H., Cassano, A., Troncoso, E., Ruby-Figueroa, R.: Prediction of permeate flux in ultrafiltration processes: A review of modeling approaches. Membranes (Basel). 11, (2021). https://doi.org/10.3390/membranes11050368
24. Wen-qiong, W., Yun-chao, W., Xiao-feng, Z., Rui-xia, G., Mao-lin, L.: Whey protein membrane processing methods and membrane fouling mechanism analysis. Food Chem. 289, 468–481 (2019). https://doi.org/10.1016/j.foodchem.2019.03.086
25. Charfi, A., Jang, H., Kim, J.: Membrane fouling by sodium alginate in high salinity conditions to simulate biofouling during seawater desalination. Bioresour. Technol. 240, 106–114 (2017). https://doi.org/10.1016/j.biortech.2017.02.086
26. Bowen, W.R., Calvo, J.I., Hernández, A.: Steps of membrane blocking in flux decline during protein microfiltration. J. Memb. Sci. 101, 153–165 (1995). https://doi.org/https://doi.org/10.1016/0376-7388(94)00295-A
27. Meng, X., Luosang, D., Meng, S., Wang, R., Fan, W., Liang, D., Li, X., Zhao, Q., Yang, L.: The structural and functional properties of polysaccharide foulants in membrane fouling. Chemosphere. 268, 129364 (2021). https://doi.org/10.1016/j.chemosphere.2020.129364
28. Rioux, L.-E., Turgeon, S.L.: Chapter 7 - Seaweed carbohydrates. Presented at the (2015)
29. Marson, G.V., Pereira, D.T.V., da Costa Machado, M.T., Di Luccio, M., Martínez, J., Belleville, M.P., Hubinger, M.D.: Ultrafiltration performance of spent brewer's yeast protein hydrolysate: Impact of pH and membrane material on fouling. J. Food Eng. 302, (2021). https://doi.org/10.1016/j.jfoodeng.2021.110569
30. She, Q., Tang, C.Y., Wang, Y.-N., Zhang, Z.: The role of hydrodynamic conditions and solution chemistry on protein fouling during ultrafiltration. Desalination. 249, 1079–1087 (2009). https://doi.org/https://doi.org/10.1016/j.desal.2009.05.015
31. Hwang, K.-J., Lin, T.-T.: Effect of morphology of polymeric membrane on the performance of cross-flow microfiltration. J. Memb. Sci. 199, 41–52 (2002). https://doi.org/https://doi.org/10.1016/S0376-7388(01)00675-5
32. Sousa, L. dos S., Cabral, B.V., Madrona, G.S., Cardoso, V.L., Reis, M.H.M.: Purification of polyphenols from green tea leaves by ultrasound assisted ultrafiltration process. Sep. Purif. Technol. 168, 188–198 (2016). https://doi.org/10.1016/j.seppur.2016.05.029

Tables

Table 1 – Kinetic models of flux decline for different fouling mechanisms for tangential filtration (Kim & DiGiano, 2009; Vela et al., 2009).

Fouling mechanism	Relationship between flux and time
Complete blocking (n=2)	Model 1: $J=(J_o-J^*)e^{-k_c J_o t}+J^*$
Intermediate pore blocking (n=1)	Model 2: $J=\frac{J_o J^* e^{k_i J^* t}}{J^*+J_o\left(e^{k_i J^* t}-1\right)}$
Internal pore blocking (n=3/2)	Model 3: $J=\frac{J_o}{\left[J_o+J_o^{1/2}\left(k_s J_o^{1/2}\right)t\right]^2}$
Cake layer formation (n=0)	Model 4: $\frac{k_g t}{J_o}=\frac{1}{J^{*2}}\left\{\left[\ln\frac{J(J_o-J^*)}{J_o(J-J^*)}\right]-J^*\left(\frac{1}{J}-\frac{1}{J_o}\right)\right\}$

Table 2 – Properties of *Fucus vesiculosus* extracts after extraction and centrifugation

	average of replicates	standard deviation
Solids' content (g/ 100 g solution)	14.31 ±	0.08
Fucose content (g/L)	3.26 ±	1.11
Iodine content (mg/L)	132 ±	3
Turbidity (NTU)	347 ±	5
L	85.81 ±	0.02
a*	-0.63 ±	0.02
b*	23.75 ±	0.01
pH	5.65 ±	0.05
Dynamic viscosity (mPa·s; 20°C)	1.73 ±	0.02

Table 3 - Properties of *Fucus vesiculosus* extract streams after ultrafiltration to a VCR of 1.33.

stream	Solids (%)	pH	L*	Cor(a*)	Cor (b*)	Turbidity (NTU)	Viscosity (mPa·s)	Flow rate (ml/min)
Permeate								
5 kDa	7.01 ± 0.80 [a]	5.76 ± 0.39 [a]	96.01 ± 2.07 [a]	-0.18 ± 0.08 [b]	2.59 ± 0.79 [a]	7 ± 7 [a]	1.06 ± 0.03 [a]	2.41 ± 0.38 [a]
50 kDa	7.85 ± 0.65 [a]	5.40 ± 0.29 [a]	95.63 ± 2.16 [a]	-0.47 ± 0.30 [a]	7.08 ± 1.85 [b]	73 ± 47 [b]	1.06 ± 0.04 [a]	3.25 ± 0.34 [b]
150 kDa	7.87 ± 1.07 [a]	5.43 ± 0.13 [a]	95.47 ± 1.67 [a]	-0.50 ± 0.13 [a]	7.74 ± 2.06 [b]	93 ± 63 [b]	1.06 ± 0.04 [a]	3.42 ± 0.44 [b]
Retentate								
5 kDa	14.93 ± 0.80 [b]	5.44 ± 0.26 [a]	84.99 ± 2.18 [b]	0.36 ± 0.55 [ab]	23.2 ± 2.43 [c]	190 ± 70 [c]	1.85 ± 0.03 [b]	
50 kDa	14.89 ± 0.65 [b]	5.47 ± 0.40 [a]	86.16 ± 2.74 [b]	0.07 ± 0.43 [ab]	25.1 ± 1.18 [cd]	267 ± 34 [d]	2.01 ± 0.07 [c]	
150 kDa	14.75 ± 0.11 [b]	5.44 ± 0.16 [a]	83.57 ± 2.93 [b]	0.54 ± 0.68 [ab]	27.9 ± 1.45 [d]	330 ± 106 [d]	1.99 ± 0.15 [c]	

Different letters means P<0.05

Table 4 - Retention coefficients on ultrafiltration of *Fucus vesiculosus* extracts

Membrane cut-off (kDa)	Solids (%)	Fucose (%)	Iodine (%)	Turbidity (%)
5	51 ± 6 [a]	35 ± 44 [a]	13 ± 9 [a]	98 ± 2 [a]
50	45 ± 5 [a]	4 ± 48 [a]	31 ± 8 [b]	77 ± 15 [b]
150	45 ± 8 [a]	64 ± 35 [a]	16 ± 11 [a]	73 ± 19 [b]

Table 5 – Parameter and determination coefficient (R^2) values from models used for flux decline at CFV=0.095 m/s and TMP=5 bar.

Model	J^*(L/m^{2}h)			J_0(L/m^{2}h)			k×10^{3*}			R^2		
	150 kDa	50 kDa	5 kDa	150 kDa	50 kDa	5 kDa	150 kDa	50 kDa	5 kDa	150 kDa	50 kDa	5 kDa
1	15.48 ±0.71	14.25 ±0.81	10.57 ±2.42	24.84 ±0.73	20.05 ±0.55	14.38 ±0.48	2.92 ±0.57	2.62 ±0.83	1.91 ±1.73	0.9758	0.9572	0.8757
2	14.95 ±0.58	13.97 ±1.03	10.33 +2.99	25.10 ±0.81	20.17 ±0.61	14.42 ±0.5	1.99 ±0.53	1.96 ±0.80	1.41 ±1.76	0.9769	0.9584	0.8776
3	-			23.07 ±0.71	19.13 ±0.42	14.14 ±0.29	0.815 ±0.107	0.592 ±0.081	0.474 ±0.082	0.9182	0.9124	0.8683
4	14.08 ±1.52	13.57 ±1.37	10.00 ±3.85	25.35 ±091	20.27 ±065	14.46 ±0.52	2.10 ±0.70	2.04 ±094	1.40 ±0.80	0.9774	0.9593	0.8793

*k=k_c (model 1 and 2 constants in m^{-1}); k=k_s (model 3 constant in $m^{-1/2}s^{-1/2}$); k=k_g (model 4 constant in s/m^2)

Table 6 – Parameter and determination coefficient (R^2) values from model 4 used for flux decline under different operating conditions.

MWCO (kDa)	CFV (m/s)	TMP (bar)	J_o(L/m^{2}h)	J*(L/m^{2}h)	$K_c \times 10^3$ (m^{-1})	R^2
150	0.081	2	24.60±1.19	10.85±2.76	5.77±2.55	0.9433
150	0.081	5	19.85±0.95	8.37±4.94	0.62±1.58	0.8709
150	0.081	8	17.66±0.66	0.08±1.89	0.46±0.094	0.8885
150	0.095	2	33.46±2.04	13.48±1.37	3.44±0.94	0.9828
150	0095	5	25.35±091	14.08±1.52	2.10±0.70	0.9774
150	0.095	8	36.16±2.27	14.65±1.12	3.86±0.95	0.9836
50	0.081	2	17.36±0.34	5.26±5.20	0.96±0.59	0.9886
50	0.081	5	29.05±1.50	12.20±1.88	2.60±0.86	0.9798
50	0.081	8	17.99±0.59	7.39±8.04	0.94±1.04	0.9584
50	0.095	2	24.37±1.77	8.96±2.91	0.96±1.50	0.8885
50	0095	5	20.27±065	13.57±1.37	2.04±094	0.9593
50	0.095	8	21.06±0.70	12.85±2.90	1.42±0.96	0.9547
5	0.081	2	9.59±0.21	2.28±0.70	0.35±2.74	0.8658
5	0.081	5	15.32±0.65	8.87±11.60	0.86±2.17	0.8408
5	0.081	8	16.02±0.89	11.16±0.56	4.93±2.26	0.9199
5	0.095	2	10.66±1.25	8.10±0.05	46.12±22.49	0.8774
5	0095	5	14.46±0.52	10.00±3.85	1.40±0.80	0.8793
5	0.095	8	16.13±0.52	10.43±1.52	2.19±1.23	0.9573

Figures

Figure 1

Predictions of fouling models to describe the variation in permeate flux with time for membranes with different molecular weight *cut-off (*MWCO), at CFV=0.095 m/s and TMP=5 bar.

Figure 2

Variation of permeate flux with time for MWCO 150, 50 and 5 kDa. Effect of cross-flow velocity (u=CFV). Fittings with model 4.

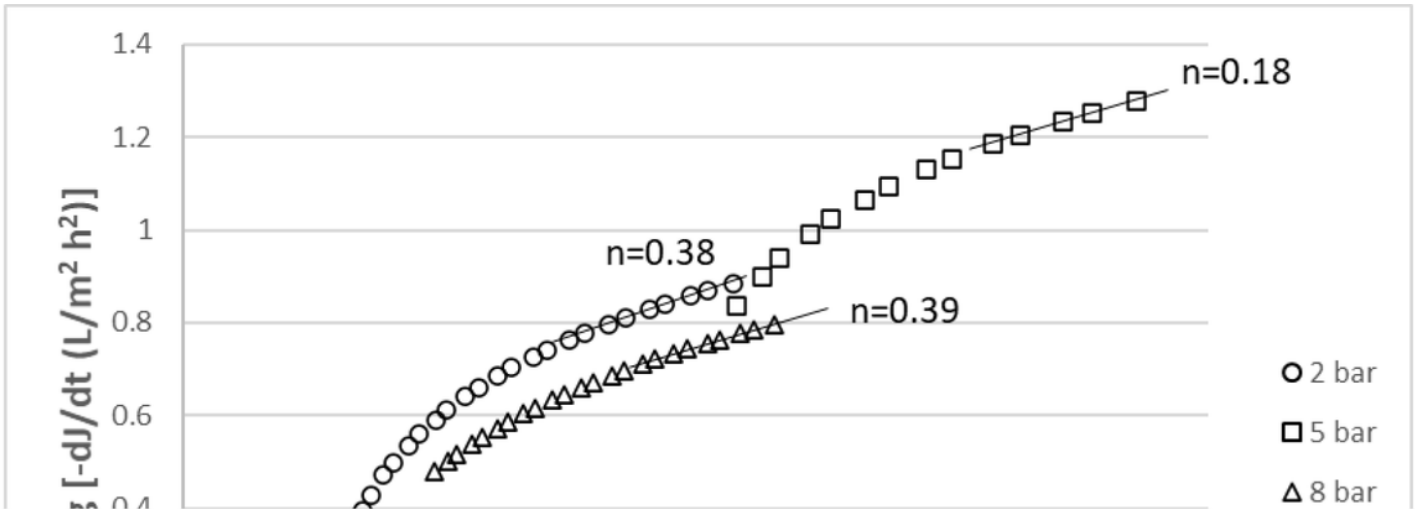

Figure 3

Filtration curve $\log(-dJ_P/dt)$ versus $\log(J_P)$ for the PESH membrane of 50 kDa and a crossflow velocity of 0.081 m/s.